

## Age-related functional changes in domain-specific medial temporal lobe pathways



David Berron<sup>a,b,\*</sup>, Katja Neumann<sup>a,b</sup>, Anne Maass<sup>b,c</sup>, Hartmut Schütze<sup>a</sup>, Klaus Fließbach<sup>d,e</sup>, Verena Kiven<sup>e</sup>, Frank Jessen<sup>f,g</sup>, Magdalena Sauvage<sup>h,i</sup>, Dharshan Kumaran<sup>j</sup>, Emrah Düzel<sup>a,b,j</sup>

<sup>a</sup> Institute of Cognitive Neurology and Dementia Research, Otto-von-Guericke University, Magdeburg, Germany

<sup>b</sup> German Center for Neurodegenerative Diseases, Magdeburg, Germany

<sup>c</sup> Helen Wills Neuroscience Institute, University of California, Berkeley, CA, USA

<sup>d</sup> University Hospital Bonn, Bonn, Germany

<sup>e</sup> German Center for Neurodegenerative Diseases, Bonn, Germany

<sup>f</sup> German Center for Neurodegenerative Diseases, Bonn-Cologne, Germany

<sup>g</sup> Department of Psychiatry, University of Cologne, Cologne, Germany

<sup>h</sup> Leibniz-Institute for Neurobiology, Functional Architecture of Memory Department, Magdeburg, Germany

<sup>i</sup> Medical Faculty, Otto-von-Guericke University, Magdeburg, Germany

<sup>j</sup> University College London, Institute of Cognitive Neuroscience, London, UK

### ARTICLE INFO

#### Article history:

Received 24 July 2017

Received in revised form 19 December 2017

Accepted 19 December 2017

Available online 31 January 2018

#### Keywords:

fMRI

Mnemonic discrimination

Aging

Entorhinal cortex

Perirhinal cortex

Hippocampus

Objects and scenes

### ABSTRACT

There is now converging evidence from studies in animals and humans that the medial temporal lobes (MTLs) harbor anatomically distinct processing pathways for object and scene information. Recent functional magnetic resonance imaging studies in humans suggest that this domain-specific organization may be associated with a functional preference of the anterior-lateral part of the entorhinal cortex (alErC) for objects and the posterior-medial entorhinal cortex (pmErC) for scenes. As MTL subregions are differentially affected by aging and neurodegenerative diseases, the question was raised whether aging may affect the 2 pathways differentially. To address this possibility, we developed a paradigm that allows the investigation of object memory and scene memory in a mnemonic discrimination task. A group of young ( $n = 43$ ) and healthy older subjects ( $n = 44$ ) underwent functional magnetic resonance imaging recordings during this novel task, while they were asked to discriminate exact repetitions of object and scene stimuli from novel stimuli that were similar but modified versions of the original stimuli (“lures”). We used structural magnetic resonance images to manually segment anatomical components of the MTL including alErC and pmErC and used these segmented regions to analyze domain specificity of functional activity. Across the entire sample, object processing was associated with activation of the perirhinal cortex (PrC) and alErC, whereas for scene processing, activation was more predominant in the parahippocampal cortex and pmErC. Functional activity related to mnemonic discrimination of object and scene lures from exact repetitions was found to overlap between processing pathways and suggests that while the PrC-alErC pathway was more involved in object discrimination, both pathways were involved in the discrimination of similar scenes. Older adults were behaviorally less accurate than young adults in discriminating similar lures from exact repetitions, but this reduction was equivalent in both domains. However, this was accompanied by significantly reduced domain-specific activity in PrC in older adults compared to what was observed in the young. Furthermore, this reduced domain-specific activity was associated to worse performance in object mnemonic discrimination in older adults. Taken together, we show the fine-grained functional organization of the MTL into domain-specific pathways for objects and scenes and their mnemonic discrimination and further provide evidence that aging might affect these pathways in a differential fashion. Future experiments will elucidate whether the 2 pathways are differentially affected in early stages of Alzheimer's disease in relation to amyloid or tau pathology.

© 2018 The Author(s). Published by Elsevier Inc. This is an open access article under the CC BY-NC-ND license (<http://creativecommons.org/licenses/by-nc-nd/4.0/>).

\* Corresponding author at: Institute of Cognitive Neurology and Dementia Research, Otto-von-Guericke University Magdeburg, House 64, Leipziger Str. 44, 39120 Magdeburg, Germany.

E-mail address: [david.berron@med.ovgu.de](mailto:david.berron@med.ovgu.de) (D. Berron).

## 1. Introduction

In the medial temporal lobe (MTL), there are domain-specific pathways that support different types of information processing and memory (Ranganath and Ritchey, 2012; Ritchey et al., 2015). The 2 pathways receive information from 2 different visual streams, which connect regions that are involved in object and spatial vision with the perirhinal cortex (PrC) and parahippocampal cortex (PhC), respectively (Kravitz et al., 2011; Mishkin et al., 1983). While the PrC is more involved in the processing of (Diana et al., 2012; Litman et al., 2009) and memory for objects and content (Davachi et al., 2003; Ekstrom and Bookheimer, 2007; Libby et al., 2014; Schultz et al., 2012; Sheldon and Levine, 2015; Staresina et al., 2011, 2013), the PhC is associated with the processing of (Diana et al., 2012; Epstein and Kanwisher, 1998; Litman et al., 2009) and memory for spatial layouts, context, and scenes (Ekstrom and Bookheimer, 2007; Libby et al., 2014; Schultz et al., 2012; Staresina et al., 2011, 2013). Studies in rodents suggest that the 2 pathways extend toward the entorhinal cortex (ErC). In rodents, the lateral ErC (LEC) is more involved in object memory and processing of local landmarks, whereas the medial ErC (MEC) is critical for spatial memory and processing of global landmarks (Knierim et al., 2014). Recent functional magnetic resonance imaging (fMRI) studies used functional connectivity analyses to investigate the human homologs of LEC and MEC in rats and found strong evidence that these subdivisions correspond to the anterior-lateral part of the entorhinal cortex (alErC) and posterior-medial entorhinal cortex (pmErC) in humans, respectively (Maass, Berron et al., 2015; Schröder, Haak et al., 2015).

The hippocampus (HC), especially the dentate gyrus (DG), plays an important role in pattern separation—a mechanism which is hypothesized to be critical for the discrimination of very similar memories (Leutgeb, 2007; Neunuebel and Knierim, 2014). Hippocampal pattern separation thereby relates to the decorrelation of similar input patterns to create distinct and independent representations that reduce the interference between these similar memories (McClelland et al., 1995; Treves and Rolls, 1992). Strong evidence for the role of the human DG in pattern separation has been shown in fMRI studies using mnemonic discrimination tasks that are likely to pose high demands on pattern separation (Bakker et al., 2008; Berron et al., 2016; Lacy et al., 2011). However, it is less clear how subregions in extrahippocampal pathways such as the PrC, PhC, and ErC are involved in mnemonic discrimination. A recent study from Reagh and Yassa showed that not only PrC and PhC but also the ErC are involved in mnemonic discrimination of similar objects and changes in object location (Reagh and Yassa, 2014). On the other hand, studies on perceptual discrimination of objects and scenes with patients who either have lesions including the PrC or the HC also suggest the involvement of extrahippocampal regions. While PrC has been shown to have a special role in the discrimination of objects with high feature overlap, the HC seems to be critically involved in scene discrimination (Barense et al., 2005; Lee et al., 2005a,b).

Mnemonic discrimination has been shown to decline with age (Stark et al., 2013; 2015). Studies using mnemonic discrimination tasks showed that older adults tend to call similar items more likely old compared to young individuals, with no difference in judging repeated items as old. This is often interpreted as a deficit in pattern separation functions and a concomitant bias toward pattern completion (Stark et al., 2015; Vieweg et al., 2015; Yassa et al., 2011a). These behavioral deficits may be related to an impairment of MTL subregions in aging as well as neurodegenerative diseases affecting the integrity of brain systems and subregions in the MTL. For example, age-related degradation in perforant pathway integrity and blood-oxygen-level dependent hyperactivity in CA3 have been associated with impairments in mnemonic discrimination (Bakker et al., 2012; Yassa et al., 2011b). However, one of the earliest

cortical sites where Alzheimer's disease (AD)-related pathology can be detected even before being evident in the HC is the trans-entorhinal region, which is part of the PrC and the ErC (Braak and Braak, 1991). This has received support by recent neuroimaging studies demonstrating a decrease in cerebral blood volume and reduced gray matter thickness in the anterior temporal lobe including the PrC and ErC in preclinical and early AD (Khan et al., 2014; Krumm et al., 2016; Yushkevich et al., 2015). Given that ErC, PrC, and PhC are critically involved in memory for objects and scenes, the impairment in PrC-alErC and PhC-pmErC can also yield degraded inputs to the HC and thus contribute to the impaired discrimination of similar lures.

To investigate age-related behavioral and functional changes related to the 2 memory domains, we developed a novel object-scene mnemonic discrimination task, which poses high demands on pattern separation. This task was designed to allow the investigation of behavioral discrimination performance as well as the neural organization of mnemonic discrimination of objects and scenes. In addition, the paradigm provides 2 potential imaging measures of functional integrity. First, we will analyze domain specificity within both MTL pathways to investigate their functional architecture as well as age-related effects. Second, we will investigate the involvement of MTL pathways in mnemonic discrimination by analyzing lure-related novelty responses based on a repetition suppression approach. In this study, we used these measures to investigate the organization and integrity of MTL pathways in a group of young as well as healthy older individuals using fMRI.

## 2. Materials and methods

### 2.1. Participants

Forty-six healthy young and 47 healthy older subjects participated in this experiment. Subjects were recruited in Bonn and Magdeburg. We excluded subjects with extensive head motion within the scanner (>2 mm [translation],  $n = 3$ ) before any functional analysis. Furthermore, we did not analyze data from subjects whose task performance was more than 2 standard deviations (SDs) below the group mean performance ( $n = 3$ ). The final sample consisted of 43 young (mean age = 24; SD = 3.5; 21 female) and 44 older subjects (mean age = 68.8; SD = 5.7; 21 female). Subjects were screened for known metabolic disorders (known history of hypertension or diabetes) and neurologic or psychiatric history and excluded from further examination in case of incidents reported during history taking. In addition, normal and corrected vision was assessed using standard procedures and printed stimulus materials comparable to the materials used during the experiments. Mini-Mental State Examination scores were available for the older group from only one site (mean score 29 [SD = 1.6]). To make sure that both older groups were comparable in cognitive performance, we statistically compared task performance of subjects with and without a Mini-Mental State Examination test score. This analysis showed no difference between the groups in object or scene discrimination performance. The study was conducted and designed in accordance with the Declaration of Helsinki (Williams, 2008) and all subjects gave informed and written consent for their participation in accordance with ethic and data security guidelines of the Otto-von-Guericke University Magdeburg and the German Center for Neurodegenerative Diseases (DZNE). The study was approved by the local ethics committees in Magdeburg and Bonn.

### 2.2. Stimuli and setting

Stimuli consisted of computer-generated (3ds Max, Autodesk Inc., San Rafael, USA) and isoluminant images. The images

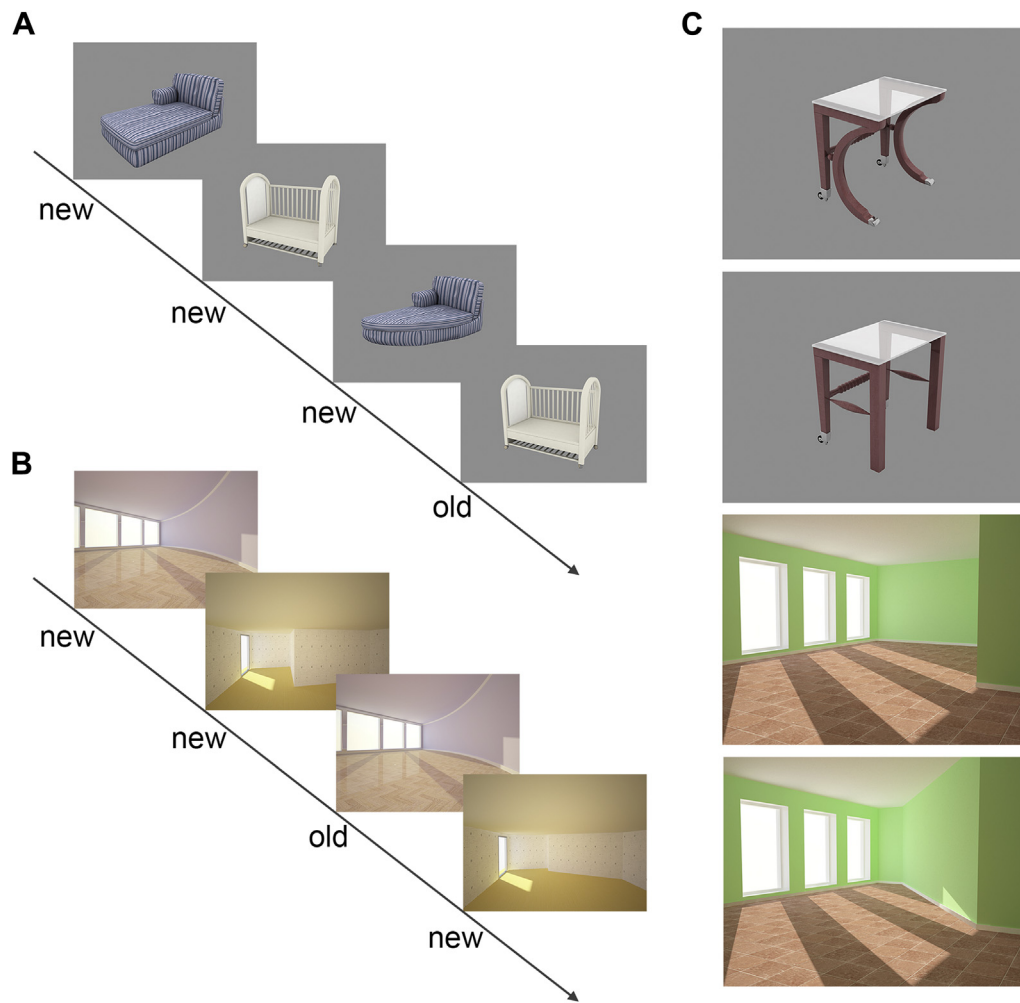


**Fig. 1.** Task sequence and stimuli. Sequences used during the object and scene paradigm. Trials consisted of 2 object (A) or scene (B) stimuli that were either identically repeated (correct response: old) or presented again in a very similar but not identical version (correct response: new). Lure and repetition stimuli only differed in shape or geometry (C).

comprised every day indoor objects presented on a gray background as well as empty indoor scenes (empty rooms, see Fig. 1). To engage different MTL processing pathways, lure stimuli were created only by changing spatial features in both stimulus categories. While we changed the local features of the objects (shape of the table leg (see Fig. 1C) but not color, position or size of the objects), we changed the global features of the rooms (geometry of the empty room but again not the color or viewpoint). Each room and object was presented 2 times where the second presentation was either an identical (repeats) or a very similar version (lures). A total of 500 self-generated stimuli were tested in behavioral experiments on young subjects ( $n = 25$ ) to define the individual stimulus lure discrimination index (i.e., the probability that subjects can differentiate between an original stimulus and its lure stimulus). In the final version of the task, the difficulty of lures and repeats was matched across domains with respect to the mean and variance. The fixation target was a white fixation star. Stimuli were presented on a fully magnetic resonance (MR)-compatible high-resolution ( $1280 \times 800$  Px) 30" LCD display (medres, Köln, Germany) and study participants watched them through a mirror mounted on the head coil, subtending a visual angle of about  $16.8^\circ$ . For experimental presentation, we used Presentation software (Neurobehavioral Systems, <https://nbs.neuro-bs.com>). Subjects' positioning in the magnetic resonance imaging (MRI) scanner as well as sequence preparation steps, for example, image angulation, was standardized

across both sites by provided standard operating procedures and on-site training.

### 2.3. Task and experimental design

Before scanning, subjects were instructed verbally and shown a standardized visual instruction with all information regarding the experiment. Subsequently, they had to learn the task within a 5-minute training session outside the scanner. In addition, a standard vision screening procedure and a visual discrimination test with stimuli comparable to the ones used in the experiment were conducted to rule out possible confounding effects of a deficit in visual perception. Vision was corrected using MR-compatible devices, if necessary. During the following fMRI session, stimuli were presented in sequences of 4 stimuli (see Fig. 1A and B) of either objects or scenes. The first 2 stimuli of a sequence were always new images, whereas the following 2 could be either an exact repetition (repeat) or a very similar version of the previous ones (lure). Stimuli were presented in an event-related design, in which each stimulus was shown for 3 seconds and stimuli were separated by a fixation star. Interstimulus intervals, ranging from 0.6 to 4.2 seconds (mean 1.63 seconds), were jittered to optimize statistical efficiency (Dale, 1999). Intervals between sequences were longer (mean 2.43 seconds) to stress the end of a sequence. Subjects had to respond to each stimulus with old/new judgments using their right index and middle fingers. Old/new

judgments were preferred over old/new/similar judgments to reduce task difficulty especially for older subjects. Subjects were told to press “new” not only for entirely new images but also for very similar versions of earlier images. “Old” responses should be given for exact repetitions. Although we consequently cannot rule out that a subject considered a similar version of an earlier stimulus as an entirely new stimulus, this was highly unlikely given the short memory delay in the task. The presentation of sequences was counterbalanced with respect to objects and scenes as well as repeats and lures. Thus, a sequence could consist of only objects or scenes but it was unpredictable for a subject whether there will be a lure or repeat pair as all possible combinations (i.e., lure-lure, repeat-repeat, repeat-lure, and lure-repeat) were counterbalanced. This resulted in a total of 56 sequences (where each sequence consists of 4 stimuli) across both domains with 56 first-repeat pairs and 56 first-lure pairs, which add up to a total of 224 object and scene trials.

#### 2.4. Behavioral data analysis

Accuracy scores and reaction times were analyzed using SPSS 24 (IBM, Armonk, USA). Hit rates (repeats percent correct), false alarm rates (lures percent incorrect) and corrected hit rates (hit rates minus false alarm rates) were calculated for the object and scene conditions. We performed a mixed analysis of variance (ANOVA) to test for differences in task accuracy with 2 within-subject factors task condition (hit rate, false alarm rate) and domain (object, scene), and the between-subject factor age group (young, older). In addition, we performed a mixed ANOVA to test for differences in reaction times for hits (correct old responses to repeats), correct rejections (correct new responses to lures), and false alarms (incorrect old responses to lures) with within-subject factors responses (hits, correct rejections, and false alarms) and domain (object, scene), and between-subject factor age group (young, older). We did not analyze reaction times for misses (incorrect new response for repeats) as there were not enough events for statistical analysis (ca. 3 events per subject).

#### 2.5. Imaging data acquisition

The study was conducted on 2 different sites, each using a 3T MRI system of the same vendor (Siemens, Erlangen, Germany) and a 32-channel head coil. Site 1 (Magdeburg) used a 3T MAGNETOM Verio with software version VB19, and site 2 (Bonn) a 3T MAGNETOM Skyra with software version VD13. At both sites, a group of young and a group of older subjects were scanned. Both sites used identical, vendor-provided sequences for the MRI acquisition. Before the fMRI session, a whole-head three-dimensional magnetization-prepared rapid acquisition gradient echo volume with 1-mm isotropic resolution, field of view =  $256 \times 256 \text{ mm}^2$ , repetition time/echo time/inversion time = 2500/4.37/1100 ms, flip angle =  $7^\circ$ , and bandwidth = 140 Hz/Px was acquired. Subsequently, 2 fMRI runs with 242 volumes each were recorded using a gradient echo echo-planar imaging sequence with  $2 \times 2 \text{ mm}^2$  in-plane resolution, field of view =  $208 \times 208 \text{ mm}^2$ , repetition time/echo time = 2400/30 ms, 10% slice gap, interleaved acquisition scheme, 40 slices with 3-mm slice thickness (young group at site 1), and 36 slices with 3.4-mm slice thickness (young group at site 2 and older groups at sites 1 and 2). Total acquisition time for each echo-planar imaging run was 12 minutes.

#### 2.6. fMRI data analyses

##### 2.6.1. Preprocessing and first level analysis

For preprocessing and statistical analyses, we used the Statistical Parametric Mapping software (SPM, Version 12; Wellcome Trust

Centre for Neuroimaging, London, UK). All functional images were corrected for differences in the time of slice acquisition and were realigned to the first image of the first session following motion estimation. The anatomical T1 image was coregistered to the mean functional image. Functional images were spatially smoothed using an isotropic Gaussian kernel of full width half maximum  $4 \times 4 \times 4 \text{ mm}$  with the purpose of increasing the signal-to-noise ratio. Images were high-pass filtered (128 seconds) to remove low-frequency signal drifts. We used a first-order autoregressive model for estimating temporal autocorrelations by using restricted maximum likelihood estimates of variance components. To model the functional data, delta functions defined by the onset of a stimulus on a trial-by-trial basis were convolved with a hemodynamic response function. First and second level data were analyzed using a mixed effect general linear model approach. All experimental conditions were entered into the general linear model as separate regressors for the following conditions: first presentations, repeats, correct lures, and incorrect lures separately for objects and scenes (i.e., 8 conditions total). Data from the first and second run were concatenated using the `spm_fmri_concatenate.m` function in SPM12. Using this function, the high-pass filtering and prewhitening were applied on a session-specific basis in the usual way. Furthermore, 6 motion parameters were added as regressors of no interest to minimize false-positive activations due to task-correlated motion (Johnstone et al., 2006). At single subject level, contrasts were created by comparing all scene and object trials (scene firsts, repeats, and lures > object firsts, repeats, and lures; and vice versa). Furthermore, we built individual contrasts for all conditions to extract region-specific t-values. To include all voxels in the MTL, an explicit mask involving gray and white matters as well as cerebrospinal fluid was used in SPM12.

##### 2.6.2. Manual delineation of MTL subregions

For each subject, anatomical masks for extrahippocampal MTL regions as well as for the HC were manually traced on T1-weighted images by 2 experienced raters. These images were coregistered to the mean echo-planar images beforehand. Masks were identified in bilateral MTL and traced on consecutive coronal slices. Segmentation was performed for each hemisphere separately using a freehand spline drawing tool based on MeVisLab (MeVis Medical Solutions AG, Bremen, Germany). This tool provided a user-friendly interface for spline drawing and editing, with which the outer borders of the masks were traced closely. The outer border contours were converted to Neuroimaging Informatics Technology Initiative images for further processing (Kuijf, 2013; Wisse et al., 2012). All Neuroimaging Informatics Technology Initiative masks were subsequently resampled to the mean functional image. Segmentation of the HC followed the European Alzheimer's Disease Consortium-Alzheimer's Disease Neuroimaging Initiative protocol (Boccardi et al., 2015). Tracing of the ErC and PrC started anteriorly at the level of the amygdala, moving caudally along the parahippocampal gyrus. At the beginning of the hippocampal body (HB), which is defined by the disappearance of the uncus apex, the posterior ErC and PrC merge into the PhC. In the anterior part, the ErC borders the amygdala nuclei medially (Fischl et al., 2009). As soon as the gyrus ambiens disappears and the hippocampal fissure opens, the ErC borders the parasubiculum medially. Laterally, the ErC borders the PrC. The edge of the medial bank of the collateral sulcus was chosen as the lateral boundary of the ErC. The ErC was further subdivided in an anterior-lateral as well as a posterior-medial section as described in Maass et al. (2015). Therefore, masks in Montreal Neurological Institute space that are available with the online version of the article were transformed to the native space of each subject and manually corrected using the protocol we suggested earlier and are described in Maass et al. (2015). PrC was defined as the region between the medial and lateral edges of the collateral sulcus (covering the medial and lateral banks).

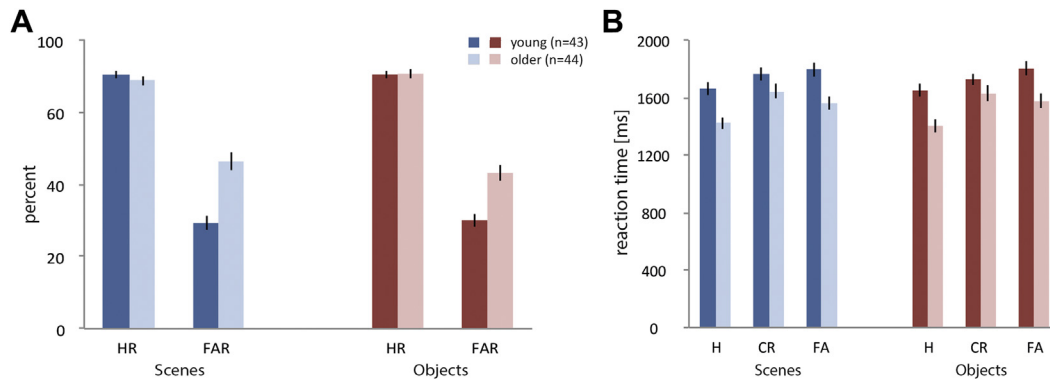


**Fig. 2.** Hit rate (HR) and false alarm rate (FAR) (A) as well as reaction times for hits (H), correct rejections (CRs), and false alarms (FA) (B) in the scene (blue) and object (red) condition for young and older subjects. (For interpretation of the references to color in this figure legend, the reader is referred to the Web version of this article.)

Segmentation of the PhC started directly posterior to the PrC and ErC. Labeling was continued posteriorly, ending on the last slice where the inferior and superior colliculi were jointly visible. The PhC was delineated as the region between subiculum (medial border) and the deepest point of the collateral sulcus (Zeineh et al., 2001). Inter-rater reliability in terms of Dice Similarity Index (Dice, 1945) was assessed in 4 hemispheres and confirmed high-to-excellent reliability ranging from 0.89 to 0.93 (HC = 0.92 [SD = 0.01]; PrC = 0.93 [SD = 0.03]; PhC = 0.89 [SD = 0.02]).

### 2.6.3. Across participant alignment (region of interest–Advanced Normalization Tools)

To enable precise cross-participant alignment for hippocampal and parahippocampal regions, first-level contrasts were normalized to a study-specific template using region of interest–Advanced Normalization Tools (Avants et al., 2011; Klein et al., 2009; Yassa and Stark, 2009). First, a study-specific template was created including all young and older participants (Avants et al., 2010). Second, regions of interest (ROIs) in the MTL were segmented manually. Therefore, hippocampal head (on the first slice on which it appears), ErC (on the first 4 consecutive slices, starting on the hippocampal head slice), HB, and PhC (same slices as HB) were labeled on the study-specific template as landmarks for the subsequent landmark-guided alignment. Similarly, subject-specific ROIs were drawn on the individual T1 images to match the template priors. Second, the expectation-based point set registration (“pse”; step size: SyN[0.5]) was used to register the individual magnetization-prepared rapid acquisition gradient echoes on the T1-template based on the labeled point sets (= ROIs). The resulting transformation matrix was then applied to each participant’s contrast image as well as to the MTL masks to verify alignment precision. Finally, the aligned contrast images were submitted to second-level group analyses. During this spatial normalization procedure, images were resampled to a resolution of  $1 \times 1 \times 1$  mm voxel size.

### 2.6.4. Group analysis

Spatially normalized first level contrasts were subjected to a second level one sample *t*-test. A regressor was added to account for the variance from the 2 different sites. Activations were thresholded at family-wise error rate (cluster)  $< 0.05$  with an initial cluster-defining threshold of  $p < 0.001$ .

### 2.6.5. ROI analysis

For ROI analyses, we extracted mean *t*-values from anatomically defined masks in the MTL. To investigate domain specificity within MTL regions, we extracted domain specificity from the scenes  $>$  objects contrast (scenes minus objects), which we refer to as domain-specificity score. Positive domain-specificity scores

indicate higher activity for scenes, whereas negative scores reflect higher activity for objects. We also investigated lure-related novelty responses, which is the difference in activity for similar lures compared to repetitions. Therefore, we extracted mean *t*-values from the correct lures  $>$  repeats contrast for objects and scenes (scene correct lures minus scene repeats; object correct lures minus object repeats). We used one-sample *t*-tests to test for domain specificity and lure-related novelty responses in PhC, PrC, as well as pmErC, alErC, and the HC. Furthermore, we used analysis of covariances (ANCOVAs) to compare difference scores and lure-related novelty responses between age groups.

Individual anatomical masks were thresholded using the implicit mask in SPM12 (0.8) before the ROI analysis. This was done to delete dropout voxels from the anatomical masks (see more information on overall dropout rates in the [Supplementary Information](#)). One older subject had severe signal dropouts specifically in alErC and therefore had to be excluded from alErC analyses.

## 3. Results

### 3.1. Behavioral performance across both task conditions

#### 3.1.1. Accuracy

For discrimination accuracies, a mixed ANOVA with the within-subject factors domain (scene and object) and measure (hit rate and false alarm rate) and the between-subjects factor age group (young and older) was performed. This mixed ANOVA showed no significant main or interaction effects for the domain, suggesting that there was no difference in accuracies between the scene and object condition neither in young nor in older subjects. However, there was a significant interaction of measure and age group ( $F_{1,85} = 36.9$ ,  $p < 0.001$ ), which was due to higher false alarm rates but not hit rates in older compared to young subjects (post hoc *t*-tests: scenes:  $M_{FARyoung} = 36.7$ ,  $M_{FARolder} = 57.9$ ,  $p < 0.001$ , objects:  $M_{FARyoung} = 37.6$ ,  $M_{FARolder} = 54$ ,  $p < 0.001$ ; see Fig. 2A). Post hoc *t*-tests also confirmed that there was no significant group difference in hit rates (scenes:  $M_{HRyoung} = 87.8$ ,  $M_{HRolder} = 86.5$ ,  $p = 0.525$ , objects:  $M_{HRyoung} = 88.12$ ,  $M_{HRolder} = 88.3$ ,  $p = 0.933$ ).

#### 3.1.2. Reaction times

We performed a mixed ANOVA with the within-subject factors domain (scene and object), condition (hit, correct rejection, and false alarm) and the between-subjects factor age group (young and older) to analyze reaction times. This mixed ANOVA showed no significant main or interaction effects for the domain, again indicating that there is no difference between the scene and object condition neither in young nor in older subjects. However, there was a significant interaction of condition and age group ( $F_{1,29,168} = 4.4$ ,  $p = 0.029$ ).

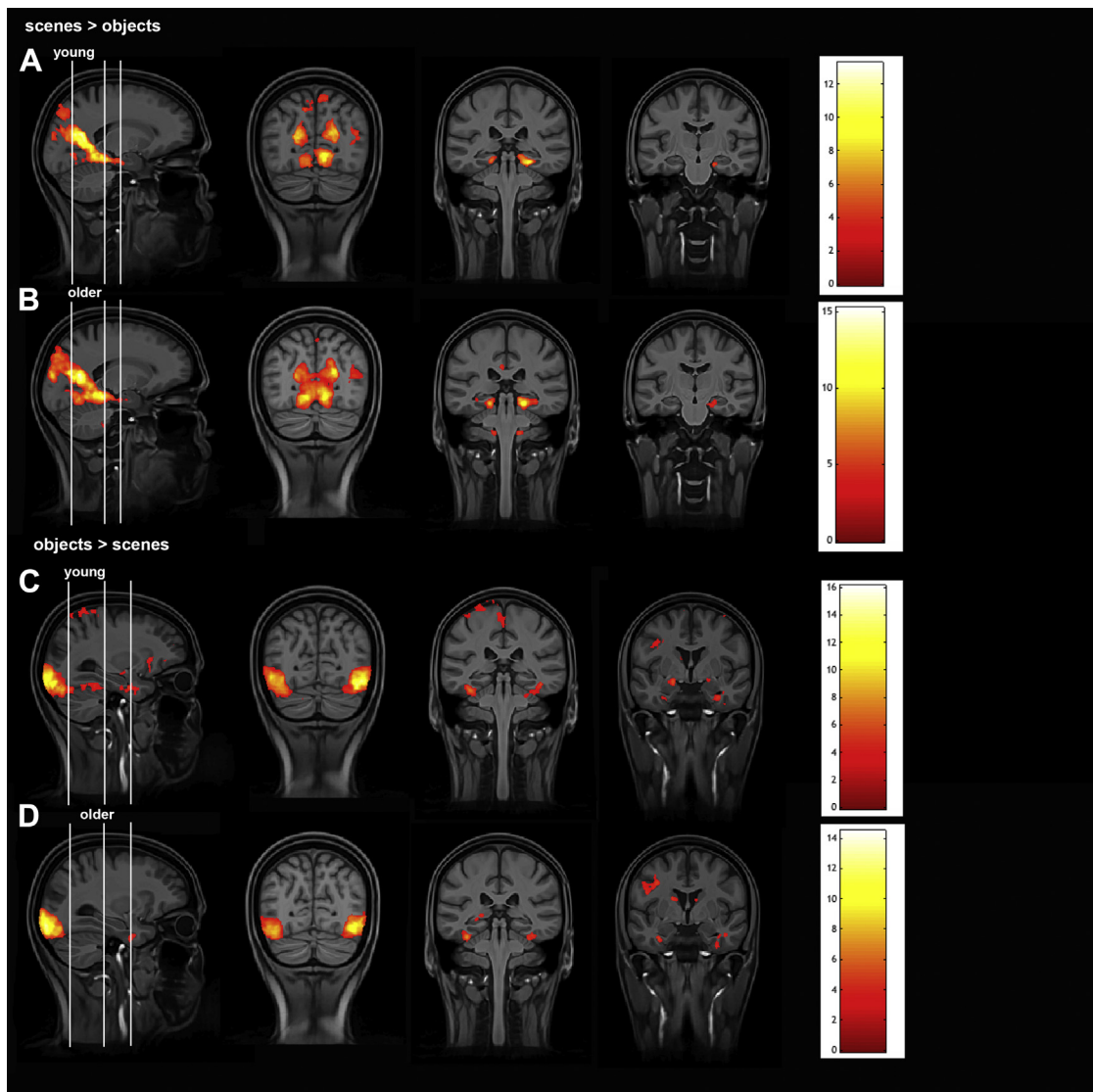


**Fig. 3.** Whole brain posterior and anterior systems associated with scene and object conditions. Scene > object (upper panel) and object > scene (lower panel) contrasts in young ( $n = 43$ , A and C) and older adults ( $n = 44$ , B and D). Results are thresholded at family-wise error rate (cluster)  $< 0.05$  with an initial cluster-defining threshold of  $p < 0.001$  and overlaid on the study-specific group template. White lines illustrate the longitudinal level of the coronal slices.

[Greenhouse-Geisser corrected]). This was due to faster reaction times associated with hits and false alarms in older compared to younger adults (post hoc t-tests: scene hits:  $M_{\text{young}} = 1.658$ ,  $M_{\text{older}} = 1.421$ ,  $p < 0.001$ , scene false alarms:  $M_{\text{young}} = 1.794$ ,  $M_{\text{older}} = 1.56$ ,  $p = 0.001$ ; object hits:  $M_{\text{young}} = 1.649$ ,  $M_{\text{older}} = 1.402$ ,  $p < 0.001$ , object false alarms:  $M_{\text{young}} = 1.802$ ,  $M_{\text{older}} = 1.575$ ,  $p = 0.002$ ) but no difference in reaction times associated to correct rejections (scene correct rejections:  $M_{\text{young}} = 1.762$ ,  $M_{\text{older}} = 1.645$ ,  $p = 0.09$ ; object correct rejections:  $M_{\text{young}} = 1.726$ ,  $M_{\text{older}} = 1.628$ ,  $p = 0.137$ ; see Fig. 2B). In addition, there was a significant effect of condition indicating that response times varied across hits, correct rejections, and false alarms ( $F_{1,29,168} = 25.8$ ,  $p = 0.000$ ).

### 3.2. Anterior-temporal and posterior-medial pathways are differentially activated in scene and object conditions

#### 3.2.1. Cortical systems are differentially involved in object and scene conditions

To investigate whether the object and scene condition in our task indeed target different cortical systems, we calculated first-level

contrast images comparing all object versus scene conditions (objects > scenes) as well as the complementary contrast where we compared all scene versus object conditions (scenes > objects) for young ( $n = 43$ ) and older subjects ( $n = 44$ ). We found that each task condition engaged specific functional pathways (see Fig. 3). While the scene condition showed higher activation in middle occipital and parietal regions, precuneus, posterior cingulum, retrosplenial cortex, PhC, cerebellum, and the subiculum, the object condition showed increased activation in middle, inferior and lateral occipital cortices, inferior parietal lobule, inferior, middle, and superior temporal gyrus, fusiform gyrus, amygdala (A), PrC, basal ganglia, the insula as well as frontal areas (see Supplementary Tables 1 and 2 for coordinates in the group-specific template space and cluster statistics for young and older subjects).

#### 3.2.2. Anterior-lateral and posterior-medial ErC are differentially involved in object and scene conditions

To investigate the 2 different pathways in more detail within the MTL, domain-specific activity in PhC and PrC, the aErC as well as the pmErC, and the HC was analyzed. A scene versus object

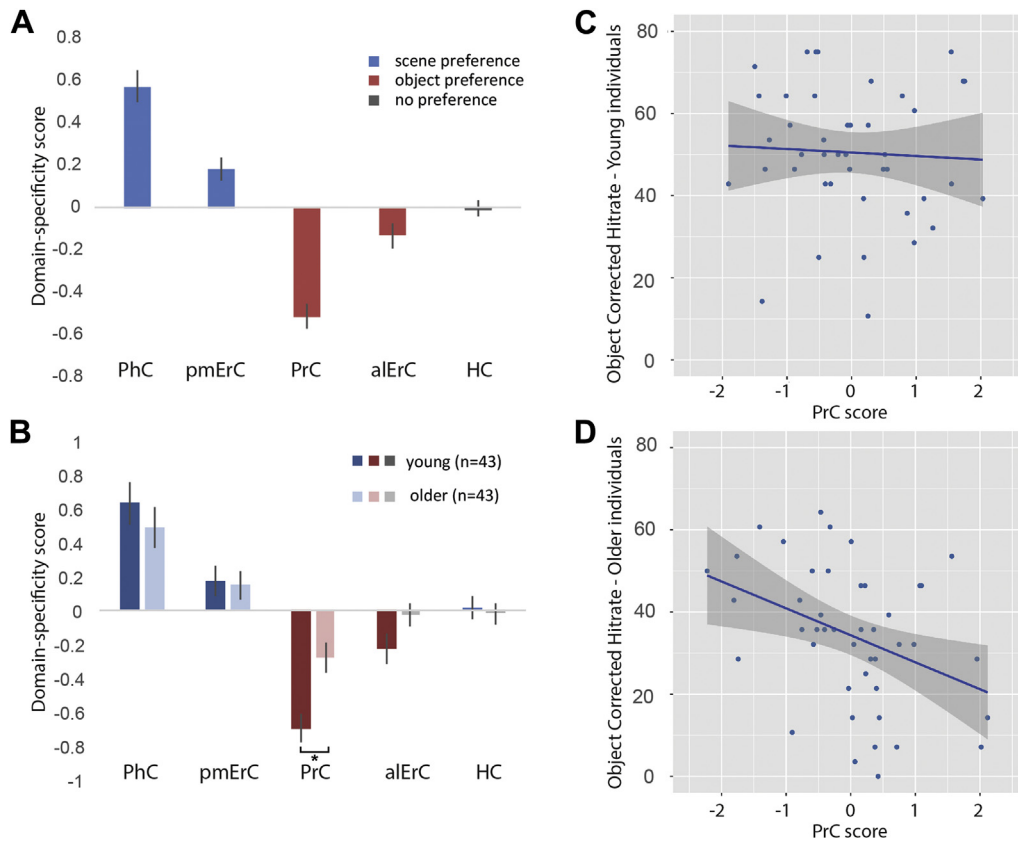


**Fig. 4.** Domain-specificity scores showing involvement in object or scene processing (mean t-values for scene condition minus object condition). Positive values indicate preferential involvement in scenes (blue), whereas negative values indicate preferential involvement in objects (red). No significant differential involvement is depicted in gray. Results are shown for the entire sample (A) as well as for young and older participants separately (B). Domain-specificity scores in PrC were significantly reduced in older individuals. The presented data are adjusted for covariates. Error bars show the standard error of the mean (SEM). \* indicates a significant group difference at  $p < 0.05$  (corrected). (C) and (D) show the relationship of the performance in the object condition and the PrC domain-specificity scores in young and older individuals, respectively. While there is no significant relationship in the young group, there is a significant negative correlation in the older individuals. Abbreviations: alErC, anterior-lateral entorhinal cortex; HC, hippocampus; PhC, parahippocampal gyrus; pmErC, posterior-medial entorhinal cortex; PrC, perirhinal cortex. (For interpretation of the references to color in this figure legend, the reader is referred to the Web version of this article.)

difference score was calculated by subtracting the t-values for all object conditions from all scene conditions. Consequently, a domain-specificity score higher than zero indicates preferential involvement of a specific region in the processing of scenes, while a score below zero indicates preferential involvement in object processing (see Fig. 4). We tested for domain-specific involvement of regions in the MTL across the entire sample, that is, young and older individuals combined, using one-sample t-tests. This revealed that PhC ( $M_{\text{PhC}} = 0.57$ , standard error of the mean [SEM] = 0.08,  $T = 7.5$ ,  $p < 0.001$ ) and pmErC ( $M_{\text{pmErC}} = 0.18$ , SEM = 0.05,  $T = 3.3$ ,  $p = 0.001$ ) were associated with domain-specificity scores significantly higher than zero suggesting preferential scene processing, while PrC ( $M_{\text{PrC}} = -0.51$ , SEM = 0.06,  $T = -8.7$ ,  $p < 0.001$ ) and alErC ( $M_{\text{alErC}} = -0.13$ , SEM = 0.06,  $T = -2.4$ ,  $p = 0.02$ ) showed scores significantly lower than zero suggesting preferential object processing. The HC ( $M_{\text{HC}} = 0.01$ , SEM = 0.04,  $T = -0.2$ ,  $p = 0.872$ ), however, did not show a domain-specificity score significantly different from zero (see Fig. 4A).

Given that perirhinal and parahippocampal cortices show strong domain-selective activity, it could be that there is blurring or bleeding from those regions into subregions of the entorhinal cortex and that this drives the results. Thus, we performed a control analysis which shows that our results are not driven by the influence of neighboring regions which can be found in the [Supplementary Information](#).

### 3.3. Age-related changes in domain specificity within MTL pathways

To compare domain-specificity scores between age groups, we performed an ANCOVA with the difference scores of all subregions (PhC, pmErC, PrC, alErC, and HC) and the factor age group (young, older). Furthermore, we added 2 covariates to account for the potential effects of different magnetic resonance (MR) scanners (scanner) as well as the different sequences (sequence). There was a significant main effect of subregion ( $F_{2,9,237} = 21.5$ ,  $p < 0.001$ ) but no significant main effect of age group ( $F_{1,82} = 0.548$ ,  $p = 0.461$ ). However, there was a significant interaction between subregion and age group ( $F_{2,9,237} = 3.7$ ,  $p = 0.006$ ). This interaction was due to reduced domain specificity as shown by post hoc t-tests in PrC ( $M_{\text{young}} = -0.67$ ,  $M_{\text{older}} = -0.36$ ,  $p = 0.007$ ) and alErC ( $M_{\text{young}} = -0.27$ ,  $M_{\text{older}} = 0$ ,  $p = 0.015$ ) in older adults, although only PrC survived Holm-Bonferroni multiple comparisons correction. No other region showed any age differences: PhC ( $M_{\text{young}} = 0.44$ ,  $M_{\text{older}} = 0.7$ ,  $p = 0.084$ ), pmErC ( $M_{\text{young}} = 0.11$ ,  $M_{\text{older}} = 0.25$ ,  $p = 0.202$ ), HC ( $M_{\text{young}} = -0.05$ ,  $M_{\text{older}} = 0.04$ ,  $p = 0.276$ ). Greenhouse-Geisser correction was used to correct for violations of sphericity where necessary. With respect to the covariates, there was no significant effect of scanner but a significant interaction of subregion and sequence ( $F_{2,9,237} = 5.1$ ,  $p < 0.002$ ). This interaction of MR sequence and subregion was due to lower domain-specificity scores

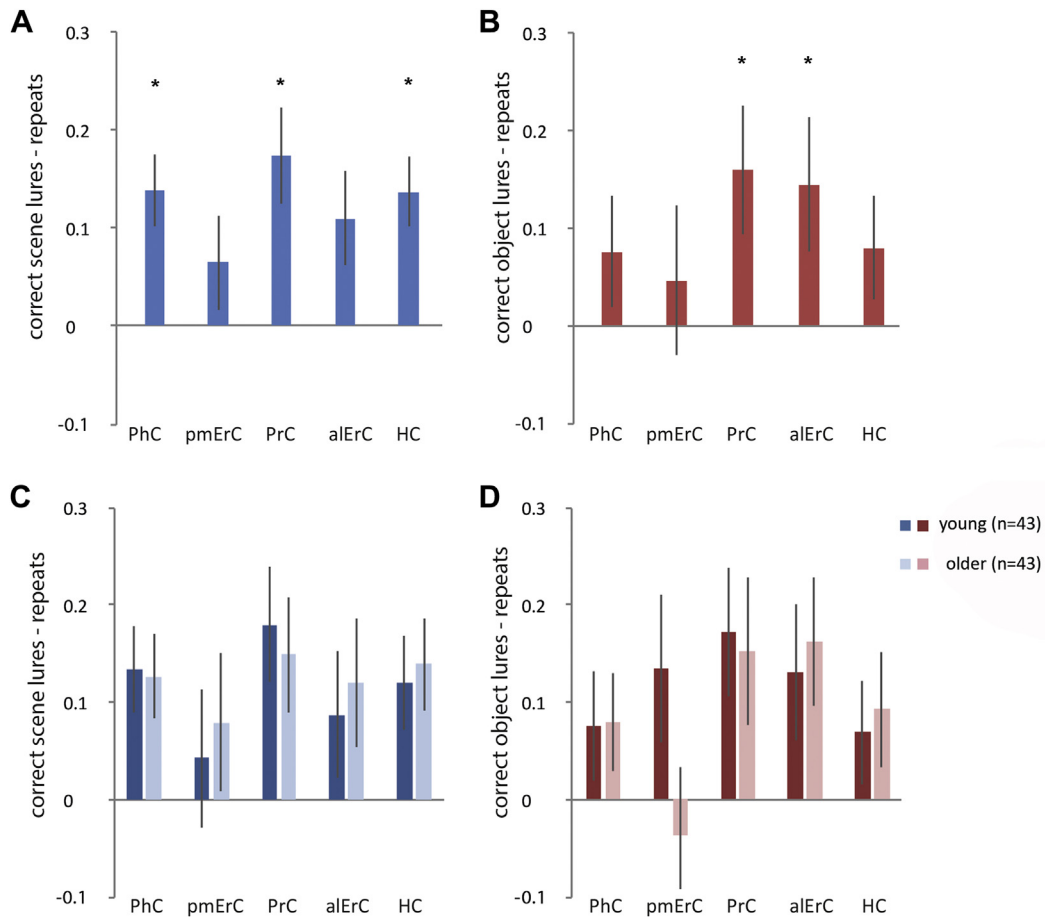


**Fig. 5.** Activity related to correctly rejected lures > repeats for scenes (blue) and objects (red) in PhC, PrC, alErC, and pmErC as well as the HC for the whole group ( $n = 87$ ) (A and B) and separately for young ( $n = 43$ ) and older participants ( $n = 44$ ) (C and D). Error bars show the standard error of the mean (SEM). Abbreviations: alErC, anterior-lateral entorhinal cortex; HC, hippocampus; PhC, parahippocampal gyrus; pmErC, posterior-medial entorhinal cortex; PrC, perirhinal cortex. \* indicates novelty responses that are significantly different from zero and survive multiple comparison correction. (For interpretation of the references to color in this figure legend, the reader is referred to the Web version of this article.)

in PhC in the young group from Magdeburg compared to the 3 other groups ( $M_{seq1} = 0.7$ ,  $M_{seq2} = 0.2$ ,  $p < 0.001$ ). There was no difference in the other subregions.

Finally, we asked whether the domain-specificity score in the PrC was related to the subjects' task performance. Therefore, we calculated Pearson correlations between z-scored domain-specificity scores in the PrC and the corrected hit rates for objects and scenes in the whole sample and separately for young and older participants. There was a significant correlation between the object-corrected hit rates and the domain-specificity scores in the PrC in older individuals ( $r = -0.383$ ,  $p = 0.010$ ) but not in young individuals ( $r = -0.053$ ,  $p = 0.737$ ) or the entire sample ( $r = -0.201$ ,  $p = 0.06$ ) (see Fig. 4C and D). There was also no significant correlation between the scene-corrected hit rates and the domain-specificity scores in the PrC in neither group (entire group:  $r = -0.107$ ,  $p = 0.326$ ; young:  $r = -0.011$ ,  $p = 0.946$ ; older:  $r = -0.256$ ,  $p = 0.094$ ). Thus, older subjects showed significantly reduced domain-specificity scores in PrC, which in turn were associated with reduced performance in object discrimination exclusively in the older age group.

#### 3.4. Lure-related novelty responses for object and scene conditions in MTL subregions

We used repetition suppression based fMRI contrasts to identify lure-related novelty responses throughout MTL subregions in all

participants. Novelty responses for similar lure trials were calculated by subtracting repeat trials from correct lure trials ("lure-related novelty," see Fig. 5). One-sample t-tests were used to test whether those difference scores were significantly different from zero. Those revealed significant lure-related novelty responses for objects in the PrC ( $M_{PrC} = 0.17$ ,  $SEM = 0.05$ ,  $T = 3.2$ ,  $p = 0.002$ ), alErC ( $M_{alErC} = 0.15$ ,  $SEM = 0.05$ ,  $T = 3$ ,  $p = 0.004$ ), the HC ( $M_{HC} = 0.08$ ,  $SEM = 0.04$ ,  $T = 2$ ,  $p = 0.049$ ), and PhC ( $M_{PhC} = 0.08$ ,  $SEM = 0.04$ ,  $T = 2$ ,  $p = 0.047$ ), although only PrC and alErC survived Holm-Bonferroni multiple comparison corrections. We did not find significant object lure-related novelty responses in pmErC ( $M_{pmErC} = 0.05$ ,  $SEM = 0.06$ ,  $T = 0.9$ ,  $p = 0.37$ ) (see Fig. 5). For scenes, we found significant novelty responses in the HC, PrC, PhC as well as alErC, although only PrC, PhC, and HC survived multiple comparison corrections ( $M_{HC} = 0.14$ ,  $SEM = 0.04$ ,  $T = 3.8$ ,  $p < 0.001$ ;  $M_{PrC} = 0.17$ ,  $SEM = 0.05$ ,  $T = 3.6$ ,  $p = 0.001$ ;  $M_{PhC} = 0.14$ ,  $SEM = 0.04$ ,  $T = 3.7$ ,  $p < 0.001$ ;  $M_{alErC} = 0.11$ ,  $SEM = 0.05$ ,  $T = 2.3$ ,  $p = 0.027$ ) (see Fig. 5A). There were no significant novelty responses in pmErC ( $M_{pmErC} = 0.07$ ,  $SEM = 0.05$ ,  $T = 1.4$ ,  $p = 0.177$ ). This suggests, while the HC, PrC, and PhC were preferentially involved in scene mnemonic discrimination, PrC and alErC were preferentially involved in object-mnemonic discrimination. However, paired t-tests between PrC and PhC as well as alErC and pmErC, respectively, could not reveal significant differences in lure-related novelty responses for neither objects nor scenes.

Finally, we performed multivariate ANCOVAs to test for group differences in lure-related novelty signals while accounting for the

potential effects of MRI scanner (scanner) and the used MR sequence (sequence). These did not reveal any age-group differences for lure-related novelty responses in objects ( $F_{1,82} = 0.8$ ,  $p = 0.362$ ) or scenes ( $F_{1,82} = 2.6$ ,  $p = 0.114$ ).

#### 4. Discussion

In this study, we investigated the functional anatomy of MTL pathways in young and healthy older individuals using a novel domain-specific mnemonic discrimination task. Crucially, regions from different cortical systems, namely the anterior-lateral and posterior-medial systems (Ranganath and Ritchey, 2012; Ritchey et al., 2015) were associated with object and scene processing, respectively. Furthermore, we found that domain-specific MTL pathways in PhC and PrC extend toward subregions in the ErC across the entire sample. While the anterior-lateral portion was more involved in object processing and memory, the posterior-medial portion was more involved in scene processing and memory. The HC, however, did not show a preference for either object or scene processing. Furthermore, investigating mnemonic discrimination across the MTL using lure-related novelty responses, PrC and alErC were involved in object discrimination, while PhC, PrC, and the HC were involved in scene discrimination. When comparing age groups, older subjects showed a diminished performance (i.e., increased false alarms) in discriminating similar lure images irrespective of the domain. In contrast to comparable lure-related novelty responses in MTL subregions (Fig. 5C and D), domain-specificity in PrC in older subjects was significantly reduced (Fig. 4B). Furthermore, this reduction in PrC domain specificity in older adults was associated with worse performance in object mnemonic discrimination.

##### 4.1. Functional organization of MTL pathways

Our findings regarding domain-specific responses in PhC and PrC fit well with earlier studies investigating material-specific processing in the MTL using object and scene stimuli. These studies showed that PhC is indeed preferentially involved in scene processing, whereas PrC is more involved in object processing (Davachi et al., 2003; Ekstrom and Bookheimer, 2007; Libby et al., 2014; Staesina et al., 2011; 2013). We extend this with our finding that differential activity extends to entorhinal subregions. Based on the functional role of the MEC and LEC in rodents, one would expect that both segments show differential involvement in the object and scene condition of our task. While MEC has a higher density of head direction and grid cells, which are modulated by spatial location and global landmarks (Hafting et al., 2005; Knierim et al., 2014; Sargolini et al., 2006), cells in LEC respond to individual objects and local landmarks (Deshmukh and Knierim, 2011; Knierim et al., 2014). Recent human studies found that strictly lateral and medial portions of the ErC showed differential activity in memory tasks. Reagh and Yassa (2014) showed that a strictly LEC portion was more involved in processing of object identity lures, whereas a strictly MEC section was more involved during a task where the object location changed on the screen (Reagh and Yassa, 2014). Similarly, Schultz et al. (2012) showed differential activity in an interference working memory task where activity in a strictly lateral and medial portion was associated with the face and scene condition, respectively. To investigate domain-specificity in the ErC, we used masks that resulted from an earlier study (Maass et al., 2015). In that study, we used intrinsic functional connectivity to investigate the human homologs of the lateral and medial entorhinal cortices described in rodents and our data suggested an alErC and pmErC portion rather than a strictly medial-lateral division. In the present study, we indeed found that pmErC was more involved

in scene processing, whereas alErC showed higher activity for the object condition. This also corroborates earlier findings from Schröder et al. (2015), who reported a similar pattern associated with the presentation of photographic object and scene stimuli. Our results therefore yield further evidence that alErC and pmErC are part of domain-specific pathways that are differentially involved in processing of objects as well as scenes.

##### 4.2. Lure-related novelty responses in the HC and extrahippocampal regions

Our results also shed light on the organization of mnemonic discrimination throughout subregions in the MTL. Earlier studies suggest that the HC, especially DG and CA3 but not other subregions in the MTL exhibit lure-related novelty responses in object (Bakker et al., 2008; Lacy et al., 2011) and also complex scene mnemonic discrimination tasks (Berron et al., 2016) that are typically viewed to be consistent with pattern separation computations. On the other hand, studies on perceptual discrimination of objects and scenes suggest that while PrC plays a critical role in discriminating objects with high feature overlap, scene discrimination mostly relies on the HC (Barense et al., 2005; Lee et al., 2005a,b). Recently, Reagh and Yassa reported extrahippocampal lure-related novelty responses in PrC, PhC, and ErC in addition to DG/CA3 in a mnemonic discrimination task of object identity as well as changes in object location (Reagh and Yassa, 2014). This suggests that lure-related novelty responses might not be limited to the HC. Indeed, in this study, we found lure-related novelty responses in the HC as well as in extrahippocampal regions. AlErC and PrC showed lure-related novelty responses for similar objects, suggesting successful mnemonic object discrimination. For scenes, we found lure-related novelty responses in PrC, PhC, and the HC. This yields evidence that while alErC-PrC are mostly contributing to mnemonic discrimination of objects, both pathways were involved in mnemonic discrimination of scenes. However, paired t-tests between PrC and PhC as well as alErC and pmErC, respectively, could not show significantly higher engagement of one pathway in one or the other condition. This finding might seem to contradict our findings of strong domain-specific responses for objects in PrC-alErC and for scenes in PhC-pmErC. A potential reason, however, might be that we limit our lure-related novelty analysis to roughly one half of the available trials, which makes it less powerful compared to the domain-specificity analysis.

On the other hand, the domain-specificity index contains information about a relative increase in activity in one compared to the other condition and does not implicate that there is no activity related to scenes in PrC. Indeed, the literature suggests that the underlying functional architecture might be more complex than a simple dichotomy (see also Connor and Knierim, 2017; Save and Sargolini, 2017 for recent reviews). A recent study in rodents indicated that object and spatial information is available in both pathways, but that this information is organized differently in LEC and MEC (Keene et al., 2016). While LEC prioritized object over location information, MEC prioritized location over object information. Another recent study reported sustained firing of perirhinal cells for spatial frames rather than only single objects (Bos et al., 2017). These findings contrast with the view that PrC contains only representations of discrete objects and would explain why we also find lure-related novelty responses for scenes in PrC.

Finally, there is also the possibility that although we designed our stimuli carefully in accordance to the findings from the animal literature, the changes in our scene lure stimuli also engage PrC. While we only changed the shape of object features to create object lures, but did not change the color or texture, we modified the overall geometry of the rooms to create scene lures. This resulted in

rather global than local feature changes in the images. Still, there is the possibility that subjects perceive the differences between original and lure scenes as feature changes, which might also engage PrC and aErC in addition to PhC and pmErC.

Furthermore, in contrast to our findings, earlier studies reported lure-related novelty responses in the HC during object as well as scene mnemonic similarity tasks (Bakker et al., 2008; 2012; Berron et al., 2016; Lacy et al., 2011; Reagh and Yassa, 2014). This contrasts with the rather weak lure-related novelty responses in the HC related to the discrimination of similar objects in our results. However, lure-related novelty responses in earlier studies were mostly limited to subregions DG and CA3 and were not evident in the remaining part of the HC. Given the resolution in the present study and the resulting limitation on subfield analyses, our results should not be taken to conclude that hippocampal subfields are not involved in mnemonic discrimination of objects. This has to be investigated in follow-up studies using high-resolution fMRI techniques. Taken together, our data suggest that visual discrimination of similar stimuli does not only depend on the HC and DG/CA3 but also involves the respective input pathways for spatial and object information.

#### 4.3. Difficulties in mnemonic discrimination of objects and scenes in aging

Our behavioral performance data show that while older subjects do not have difficulties to identify repeated images, they have problems to identify similar lures. This has been already reported by other studies showing impairment in tasks that are meant to tax object pattern separation (Pidgeon and Morcom, 2014; Stark et al., 2013; Yassa et al., 2011a) as well as spatial pattern separation (Holden and Gilbert, 2012; Holden et al., 2012; Stark et al., 2010). In addition, our reaction time data suggest that older subjects have a bias toward “old” responses indicated by faster reaction times for false alarms and hits in contrast to correct rejections. This bias could also imply a higher percentage of guesses within the correct hits of older participants. Although we are unable to quantify this proportion, there is the possibility that older subjects have also difficulties to identify hits.

Several recent studies investigated whether object or spatial discrimination is more sensitive to aging. Reagh and Yassa used a task in which they compared the performance of young and older subjects in detecting changes in object identity compared to a change in object location (Reagh et al., 2016). They found that older individuals with and without impairment in verbal memory (Rey Auditory Verbal Learning Test, delayed recall) showed different performance profiles in a mnemonic discrimination task. While nonimpaired subjects showed difficulties limited to object identity discrimination, the impaired older subjects showed difficulties in both the object identity and change-in-object-location task. Following a similar approach, Johnson et al. reported age-related deficits in object discrimination in rodents. Although they did not use spatial learning and object memory tasks that were equally matched in task difficulty, they reported less impairment in the spatial compared to the object domain in the same animals (Johnson et al., 2017). Another recent study reported that test scores in the Montreal Cognitive Assessment battery in older adults shared a stronger association with object memory than memory for scenes (Fidalgo et al., 2016), which suggests that already impaired older subjects show predominant impairment in object memory. Although this indicates that object discrimination might indeed be more sensitive to aging, so far there is no study yet showing differences in difficulty-matched object and scene tasks in older adults. Our results show that while healthy older subjects are impaired in discriminating similar images, this impairment is not specific to objects or scenes. This is further corroborated

by a recent study from Stark and Stark in which they compared discrimination performance between young and older subjects in 2 mnemonic similarity tasks—one using objects and one using scenes (Stark and Stark, 2017). The tasks had notable differences compared to ours as their lure stimuli varied on various dimensions including size, color orientation, and position. In addition, the scenes used in their task contained various objects that could be subject to change in their similar counterpart. However, older subjects again showed an overall impairment in lure discrimination in the object as well as in the scene task.

#### 4.4. Functional integrity of anterior-temporal and posterior-medial pathways

To investigate age-related functional changes in both medial temporal pathways, we compared domain-specificity scores as well as lure-related novelty signals between age groups. Lure-related novelty responses were evident in older subjects for both objects and scenes, and we did not find evidence for differences between age groups. However, domain-specificity scores showed that there was a significant reduction in domain-specificity in PrC of older compared to young individuals. We found a similar but weaker result in aErC, which also showed reduced domain specificity but did not survive multiple comparison correction.

In aging research, it is always difficult to know whether this reduction of domain specificity is related to impairment or rather task difficulty mirrored by reduced performance and therefore less correct trials. However, in this case, the domain-specificity analysis is done using all object and scene trials, which likely limits the influence of correct trials. In addition, there are differences in the behavioral performance of young and older subjects in both object and scene conditions. However, we only see a significant group difference specifically in PrC but not in PhC or pmErC. If this result would reflect difficulty per se, we would expect a similar reduction in PhC or pmErC. Finally, we found a significant correlation between the performance in object mnemonic discrimination and domain-specificity scores in PrC in older individuals but not in the young group. This means that although there are some young participants that had difficulties with the task, this was not associated with the domain-specificity score. Thus, we believe that our results rather indicate impairment in the older group. Earlier neuroimaging studies also reported similar findings. While Ryan et al. reported reduced activity in PrC of older adults in an object discrimination task which was specifically associated with lower performance in the discrimination of objects that shared high feature overlap (Ryan et al., 2012), Reagh et al. (2017) showed that reduced aErC activity was related to worse object mnemonic discrimination.

Although our sample of older adults was seemingly healthy, it is likely that several of these older participants already harbor tau pathology in their MTLs (Braak and Braak, 1991). Due to the lack of cerebrospinal fluid and PET biomarkers of Alzheimer's pathology in our study, we cannot quantify this proportion. Postmortem data point to the lateral ErC and PrC as the first cortical regions to accumulate tau neurofibrillary tangles in AD (Braak and Tredici, 2012). More specifically, tau deposits in the transentorhinal region (Braak stages I/II), which is part of the PrC, are common in individuals aged 60 years and above (>60%) and are considered as silent, preclinical stages of AD (Braak and Braak, 1997). In accordance with the neuropathological data, a study demonstrated that preclinical AD patients (progressors vs. nonprogressors) showed already reduced cerebral blood volume measures in the lateral entorhinal, transentorhinal, and perirhinal cortices (Khan et al., 2014). Recent structural MRI studies could also detect early structural alterations in perirhinal and lateral entorhinal cortices in aging (Olsen et al., 2017) and early stages of AD (Krumm et al., 2016; Miller et al., 2015; Wolk

et al., 2017; Yushkevich et al., 2015). Thus, reduced domain specificity in PrC and domain-agnostic activity in aErC could be an early indicator of functional impairment in MTL pathways.

Taken together, we show functional domain specificity in PrC-aErC and PhC-pmErC for objects and scenes, respectively. In addition, we show lure-related novelty signals associated with the discrimination of similar objects and scenes. While lure-related novelty responses in MTL subregions are maintained in old age, domain specificity is reduced in PrC and aErC, and this reduction in PrC is associated with worse object mnemonic discrimination in older adults. Thus, our data suggest that aging might affect the MTL object pathway disproportionately strong—with a deficit in mnemonic discrimination associated with aging in both domains. It will be important to relate the functional and behavioral underpinnings of domain-specific memory processing to preclinical AD pathology to understand whether pathology is associated with a domain-selective impairment.

### Disclosure statement

The authors have no actual or potential conflicts of interest.

### Acknowledgements

The authors thank Michael Scholz for help with the statistical optimization of the experimental design. The authors also thank Yi Chen and Jonathan Shine for valuable discussions of the article. ED was supported by DFG grant: SFB779 A07. ED and DB are scientific co-founders of neotiv GmbH.

### Appendix A. Supplementary data

Supplementary data associated with this article can be found, in the online version, at <https://doi.org/10.1016/j.neurobiolaging.2017.12.030>.

### References

- Avants, B.B., Tustison, N.J., Song, G., Cook, P.A., Klein, A., Gee, J.C., 2011. A reproducible evaluation of ANTs similarity metric performance in brain image registration. *NeuroImage* 54, 2033–2044.
- Avants, B.B., Yushkevich, P., Pluta, J., Minkoff, D., Korczynowski, M., Detre, J., Gee, J.C., 2010. The optimal template effect in hippocampus studies of diseased populations. *NeuroImage* 49, 2457–2466.
- Bakker, A., Kirwan, C.B., Miller, M., Stark, C., 2008. Pattern separation in the human hippocampal CA3 and dentate gyrus. *Science* 319, 1640–1642.
- Bakker, A., Krauss, G.L., Albert, M.S., Speck, C.L., Jones, L.R., Stark, C.E., Yassa, M.A., Bassett, S.S., Shelton, A.L., Gallagher, M., 2012. Reduction of hippocampal hyperactivity improves cognition in amnesic mild cognitive impairment. *Neuron* 74, 467–474.
- Barense, M., Bussey, T.J., Lee, A.C., Rogers, T.T., Davies, R.R., Saksida, L.M., Murray, E.A., Graham, K.S., 2005. Functional specialization in the human medial temporal lobe. *J. Neurosci.* 25, 10239–10246.
- Berron, D., Schütze, H., Maass, A., Cardenas-Blanco, A., Kuijff, H., Kumaran, D., Düzel, E., 2016. Strong evidence for pattern separation in human dentate gyrus. *J. Neurosci.* 36, 7569–7579.
- Boccardi, M., Bocchetta, M., Apostolova, L.G., Barnes, J., Bartzokis, G., Corbetta, G., DeCarli, C., deToledo-Morrell, L., Firbank, M., Ganzola, R., Gerritsen, L., Henneman, W., Killiany, R.J., Malykhin, N., Pasqualetti, P., Pruessner, J.C., Redolfi, A., Robitaille, N., Soininen, H., Tolomeo, D., Wang, L., Watson, C., Wolf, H., Duvernoy, H., Duchesne, S., Jack Jr., C.R., Frisoni, G.B., 2015. EADC-ADNI Working Group on the Harmonized Protocol for Manual Hippocampal Segmentation, Delphi definition of the EADC-ADNI Harmonized Protocol for hippocampal segmentation on magnetic resonance. *Alzheimers Dement.* 11, 126–138.
- Bos, J., Vinck, M., van Mourik-Donga, L., Jackson, J., Witter, M., Pennartz, C., 2017. Perirhinal firing patterns are sustained across large spatial segments of the task environment. *Nat. Commun.* 8, 15602.
- Braak, H., Braak, E., 1991. Demonstration of amyloid deposits and neurofibrillary changes in whole brain sections. *Brain Pathol.* 1, 213–216.
- Braak, H., Braak, E., 1997. Frequency of stages of Alzheimer-related lesions in different age categories. *Neurobiol. Aging* 18, 351–357.
- Braak, H., Tredici, K., 2012. Alzheimer's disease: pathogenesis and prevention. *Alzheimer's Dement.* 8, 227–233.
- Connor, C., Knierim, J., 2017. Integration of objects and space in perception and memory. *Nat. Neurosci.* 20, 1493–1503.
- Dale, A.M., 1999. Optimal experimental design for event-related fMRI. *Hum. Brain Mapp.* 8, 109–114.
- Davachi, L., Mitchell, J., Wagner, A., 2003. Multiple routes to memory: distinct medial temporal lobe processes build item and source memories. *Proc. Natl. Acad. Sci. U. S. A.* 100, 2157–2162.
- Deshmukh, S., Knierim, J., 2011. Representation of non-spatial and spatial information in the lateral entorhinal cortex. *Front. Behav. Neurosci.* 5, 69.
- Diana, R., Yonelinas, A., Ranganath, C., 2012. Adaptation to cognitive context and item information in the medial temporal lobes. *Neuropsychologia* 50, 3062–3069.
- Dice, L., 1945. Measures of the amount of ecologic association between species. *Ecology* 26, 297–302.
- Ekstrom, A., Bookheimer, S., 2007. Spatial and temporal episodic memory retrieval recruit dissociable functional networks in the human brain. *Learn. Mem.* 14, 645–654.
- Epstein, R., Kanwisher, N., 1998. A cortical representation of the local visual environment. *Nature* 392, 598–601.
- Fidalgo, C., Changoor, A., Page-Gould, E., Lee, A., Barense, M., 2016. Early cognitive decline in older adults better predicts object than scene recognition performance. *Hippocampus* 26, 1579–1592.
- Fischl, B., Stevens, A., Rajendran, N., Yeo, T., Greve, D., Leemput, K., Polimeni, J., Kakunoori, S., Buckner, R., Pacheco, J., Salat, D., Melcher, J., Frosch, M., Hyman, B., Grant, E., Rosen, B., van der Kouwe, A., Wiggins, G., Wald, L., Augustinack, J., 2009. Predicting the location of entorhinal cortex from MRI. *NeuroImage* 47, 8–17.
- Hafting, T., Fyhn, M., Molden, S., Moser, M.-B., Moser, E., 2005. Microstructure of a spatial map in the entorhinal cortex. *Nature* 436, 801–806.
- Holden, H., Gilbert, P., 2012. Less efficient pattern separation may contribute to age-related spatial memory deficits. *Front. Aging Neurosci.* 4, 9.
- Holden, H., Hoebel, C., Loftis, K., Gilbert, P., 2012. Spatial pattern separation in cognitively normal young and older adults. *Hippocampus* 22, 1826–1832.
- Johnson, S., Turner, S., Santacrose, L., Carty, K., Shafiq, L., Bizoz, J., Maurer, A., Burke, S., 2017. Age-related impairments in discriminating perceptually similar objects parallel those observed in humans. *Hippocampus* 27, 759–776.
- Johnstone, T., Ores Walsh, K.S., Greischar, L.L., Alexander, A.L., Fox, A.S., Davidson, R.J., Oakes, T.R., 2006. Motion correction and the use of motion covariates in multiple subject fMRI analysis. *Hum. Brain Mapp.* 27, 779–788.
- Keene, C., Bladon, J., McKenzie, S., Liu, C., O'Keefe, J., Eichenbaum, H., 2016. Complementary functional organization of neuronal activity patterns in the perirhinal, lateral entorhinal, and medial entorhinal cortices. *J. Neurosci.* 36, 3660–3675.
- Khan, U., Liu, L., Provenzano, F., Berman, D., Profaci, C., Sloan, R., Mayeux, R., Duff, K., Small, S., 2014. Molecular drivers and cortical spread of lateral entorhinal cortex dysfunction in preclinical Alzheimer's disease. *Nat. Neurosci.* 17, 304–311.
- Klein, A., Andersson, J., Ardekani, B.A., Ashburner, J., Avants, B., Chiang, M.C., Christensen, G.E., Collins, D.L., Gee, J., Hellier, P., Song, J.H., Jenkinson, M., Lepage, C., Rueckert, D., Thompson, P., Vercauteren, T., Woods, R.P., Mann, J.J., Parsey, R.V., 2009. Evaluation of 14 nonlinear deformation algorithms applied to human brain MRI registration. *NeuroImage* 46, 786–802.
- Knierim, J., Neunuebel, J., Deshmukh, S., 2014. Functional correlates of the lateral and medial entorhinal cortex: objects, path integration and local–global reference frames. *Philos. Trans. R. Soc. Lond. B Biol. Sci.* 369, 20130369.
- Kravitz, D., Saleem, K., Baker, C., Mishkin, M., 2011. A new neural framework for visuospatial processing. *Nat. Rev. Neurosci.* 12, 217–230.
- Krumm, S., Kivisaari, S., Probst, A., Monsch, A., Reinhardt, J., Ulmer, S., Stippich, C., Kressig, R., Taylor, K., 2016. Cortical thinning of parahippocampal subregions in very early Alzheimer's disease. *Neurobiol. Aging* 38, 188–196.
- Kuijff, H.J., 2013. Image Processing Techniques for Quantification and Assessment of Brain MRI. Utrecht University, Utrecht.
- Lacy, J., Yassa, M., Stark, S., Muftuler, T., Stark, C., 2011. Distinct pattern separation related transfer functions in human CA3/dentate and CA1 revealed using high-resolution fMRI and variable mnemonic similarity. *Learn. Mem.* 18, 15–18.
- Lee, A., Barense, M., Graham, K., 2005a. The contribution of the human medial temporal lobe to perception: bridging the gap between animal and human studies. *Q. J. Exp. Psychol. B* 58, 300–325.
- Lee, A., Bussey, T.J., Murray, E.A., Saksida, L.M., Epstein, R.A., Kapur, N., Hodges, J.R., Graham, K.S., 2005b. Perceptual deficits in amnesia: challenging the medial temporal lobe 'mnemonic' view. *Neuropsychologia* 43, 1–11.
- Leutgeb, S., Leutgeb, J., 2007. Pattern separation, pattern completion, and new neuronal codes within a continuous CA3 map. *Learn. Mem.* 14, 745–757.
- Libby, L., Hannula, D., Ranganath, C., 2014. Medial temporal lobe Coding of item and spatial information during relational binding in working memory. *J. Neurosci.* 34, 14233–14242.
- Litman, L., Awipi, T., Davachi, L., 2009. Category-specificity in the human medial temporal lobe cortex. *Hippocampus* 19, 308–319.
- Maass, A., Berron, D., Libby, L., Ranganath, C., Düzel, E., 2015. Functional subregions of the human entorhinal cortex. *Elife* 4.
- McClelland, J., McNaughton, B., O'Reilly, R., 1995. Why there are complementary learning systems in the hippocampus and neocortex: insights from the successes and failures of connectionist models of learning and memory. *Psychol. Rev.* 102, 419–457.
- Miller, M., Ratnanather, T., Tward, D., Brown, T., Lee, D., Ketcha, M., Mori, K., Wang, M.-C., Mori, S., Albert, M., Younes, L., Team, B., 2015. Network

- neurodegeneration in Alzheimer's disease via MRI based shape diffeomorphic and high-field atlas. *Front. Bioeng. Biotechnol.* 3, 54.
- Mishkin, M., Ungerleider, L., Macko, K., 1983. Object vision and spatial vision: two cortical pathways. *Trends Neurosci.* 6, 414–417.
- Neunuebel, J., Knierim, J., 2014. CA3 retrieves coherent representations from degraded input: direct evidence for CA3 pattern completion and dentate gyrus pattern separation. *Neuron* 81, 416–427.
- Olsen, R.K., Yeung, L.-K., Noly-Gandon, A., D'Angelo, M.C., Kacollja, A., Smith, V.M., Ryan, J.D., Barense, M.D., 2017. Human anterolateral entorhinal cortex volumes are associated with cognitive decline in aging prior to clinical diagnosis. *Neurobiol. Aging* 57, 195–205.
- Pidgeon, L., Morcom, A., 2014. Age-related increases in false recognition: the role of perceptual and conceptual similarity. *Front. Aging Neurosci.* 6, 283.
- Ranganath, C., Ritchey, M., 2012. Two cortical systems for memory-guided behaviour. *Nat. Rev. Neurosci.* 13, 713–726.
- Reagh, Z., Yassa, M., 2014. Object and spatial mnemonic interference differentially engage lateral and medial entorhinal cortex in humans. *Proc. Natl. Acad. Sci. U. S. A.* 111, E4264–E4273.
- Reagh, Z.M., Ho, H.D., Leal, S.L., Noche, J.A., Chun, A., Murray, E.A., Yassa, M.A., 2016. Greater loss of object than spatial mnemonic discrimination in aged adults. *Hippocampus* 26, 417–422.
- Reagh, Z.M., Noche, J.A., Tustison, N., Delisle, D., Murray, E.A., Yassa, M.A., 2017. Anterolateral entorhinal-hippocampal imbalance in older adults disrupts object pattern separation. *bioRxiv preprint that has not been peer-reviewed.*
- Ritchey, M., Libby, L., Ranganath, C., 2015. Cortico-hippocampal systems involved in memory and cognition: the PMAT framework. *Prog. Brain Res.* 219, 45–64.
- Ryan, L., Cardoza, J.A., Barense, M.D., Kawa, K.H., Wallentin-Flores, J., Arnold, W.T., Alexander, G.E., 2012. Age-related impairment in a complex object discrimination task that engages perirhinal cortex. *Hippocampus* 22, 1978–1989.
- Sargolini, F., Fyhn, M., Hafting, T., McNaughton, B., Witter, M., Moser, M.-B., Moser, E., 2006. Conjunctive representation of position, direction, and velocity in entorhinal cortex. *Science* 312, 758–762.
- Save, E., Sargolini, F., 2017. Disentangling the role of the MEC and LEC in the processing of spatial and non-spatial information: contribution of lesion studies. *Front. Syst. Neurosci.* 11, 81.
- Schröder, T., Haak, K., Jimenez, N., Beckmann, C., Doeller, C., 2015. Functional topography of the human entorhinal cortex. *eLife* 4.
- Schultz, H., Sommer, T., Peters, J., 2012. Direct evidence for domain-sensitive functional subregions in human entorhinal cortex. *J. Neurosci.* 32, 4716–4723.
- Sheldon, S., Levine, B., 2015. The medial temporal lobes distinguish between within-item and item-context relations during autobiographical memory retrieval. *Hippocampus* 25, 1577–1590.
- Staresina, B., Duncan, K., Davachi, L., 2011. Perirhinal and parahippocampal cortices differentially contribute to later recollection of object- and scene-related event details. *J. Neurosci.* 31, 8739–8747.
- Staresina, B., Cooper, E., Henson, R., 2013. Reversible information flow across the medial temporal lobe: the Hippocampus links cortical modules during memory retrieval. *J. Neurosci.* 33, 14184–14192.
- Stark, S., Stark, C., 2017. Age-related deficits in the mnemonic similarity task for objects and scenes. *Behav. Brain Res.* 333, 109–117.
- Stark, S., Yassa, M., Stark, C., 2010. Individual differences in spatial pattern separation performance associated with healthy aging in humans. *Learn. Mem.* 17, 284–288.
- Stark, S., Yassa, M., Lacy, J., Stark, C., 2013. A task to assess behavioral pattern separation (BPS) in humans: data from healthy aging and mild cognitive impairment. *Neuropsychologia* 51, 2442–2449.
- Stark, S., Stevenson, R., Wu, C., Rutledge, S., Stark, C., 2015. Stability of age-related deficits in the mnemonic similarity task across task variations. *Behav. Neurosci.* 129, 257–268.
- Treves, A., Rolls, E., 1992. Computational constraints suggest the need for two distinct input systems to the hippocampal CA3 network. *Hippocampus* 2, 189–199.
- Vieweg, P., Stangl, M., Howard, L., Wolbers, T., 2015. Changes in pattern completion – a key mechanism to explain age-related recognition memory deficits? *Cortex* 64, 343–351.
- Williams, J.R., 2008. The Declaration of Helsinki and public health. *Bull. World Health Organ.* 86, 650–652.
- Wisse, L.E.M., Gerritsen, L., Zwanenburg, J.J.M., Kuijf, H.J., Luijten, P.R., Biessels, G.J., Geerlings, M.I., 2012. Subfields of the hippocampal formation at 7T MRI: in vivo volumetric assessment. *NeuroImage* 61, 1043–1049.
- Wolk, D., Das, S., Mueller, S., Weiner, M., Yushkevich, P., Initiative, A., 2017. Medial temporal lobe subregional morphometry using high resolution MRI in Alzheimer's disease. *Neurobiol. Aging* 49, 204–213.
- Yassa, M., Lacy, J., Stark, S., Albert, M., Gallagher, M., Stark, C., 2011a. Pattern separation deficits associated with increased hippocampal CA3 and dentate gyrus activity in nondemented older adults. *Hippocampus* 21, 968–979.
- Yassa, M., Mattfeld, A., Stark, S., Stark, C., 2011b. Age-related memory deficits linked to circuit-specific disruptions in the hippocampus. *Proc. Natl. Acad. Sci.* 108, 8873–8878.
- Yassa, M., Stark, C., 2009. A quantitative evaluation of cross-participant registration techniques for MRI studies of the medial temporal lobe. *NeuroImage* 44, 319–327.
- Yushkevich, P., Pluta, J., Wang, H., Xie, L., Ding, S., Gertje, E., Mancuso, L., Kliot, D., Das, S., Wolk, D., 2015. Automated volumetry and regional thickness analysis of hippocampal subfields and medial temporal cortical structures in mild cognitive impairment. *Hum. Brain Mapp.* 36, 258–287.
- Zeineh, M., Engel, S., Thompson, P., Bookheimer, S., 2001. Unfolding the human hippocampus with high resolution structural and functional MRI. *Anatomical Rec.* 265, 111–120.